Determination of strain fields in porous shape memory alloys using micro computed tomography

Therese Bormann[a,b,c], Sebastian Friess*[d], Michael de Wild[b], Ralf Schumacher[b], Georg Schulz[a], and Bert Müller[a,c]

[a]Biomaterials Science Center, University of Basel, 4031 Basel, Switzerland;
[b]School of Life Sciences, University of Applied Sciences Northwestern Switzerland, 4032 Muttenz, Switzerland;
[c]School of Dental Medicine, University of Basel, 4056 Basel, Switzerland;
[d]Gloor Instruments AG, 8610 Uster, Switzerland

ABSTRACT

Shape memory alloys (SMAs) belong to 'intelligent' materials since the metal alloy can change its macroscopic shape as the result of the temperature-induced, reversible martensite-austenite phase transition. SMAs are often applied for medical applications such as stents, hinge-less instruments, artificial muscles, and dental braces. Rapid prototyping techniques, including selective laser melting (SLM), allow fabricating complex porous SMA microstructures. In the present study, the macroscopic shape changes of the SMA test structures fabricated by SLM have been investigated by means of micro computed tomography (μCT). For this purpose, the SMA structures are placed into the heating stage of the μCT system SkyScan 1172™ (SkyScan, Kontich, Belgium) to acquire three-dimensional datasets above and below the transition temperature, i.e. at room temperature and at about 80 °C, respectively. The two datasets were registered on the basis of an affine registration algorithm with nine independent parameters – three for the translation, three for the rotation and three for the scaling in orthogonal directions. Essentially, the scaling parameters characterize the macroscopic deformation of the SMA structure of interest. Furthermore, applying the non-rigid registration algorithm, the three-dimensional strain field of the SMA structure on the micrometer scale comes to light. The strain fields obtained will serve for the optimization of the SLM-process and, more important, of the design of the complex shaped SMA structures for tissue engineering and medical implants.

Keywords: Shape memory alloy, selective laser melting, micro computed tomography, heating stage, registration, strain field

1. INTRODUCTION

Shape memory alloys are often termed 'intelligent' materials because of their ability to pre-defined shape changes. For some specific alloys, one finds thermally or mechanically induced solid-solid phase transitions without significant atom diffusion. One of the best-known SMAs is the binary NiTi alloy with a composition of about 50:50 at%, which changes its shape via a crystalline transition from martensite to austenite and vice versa. Its low temperature martensite phase is associated with a monoclinic structure and the high temperature austenite phase with a body-centered cubic phase.[1] Changing the composition, i.e. the Ni-Ti ratio, the temperature range of the phase transition can be adjusted between -150 °C and 100 °C.[2] As the body temperature lies within this temperature range, the properties of NiTi SMAs are important for numerous medical applications.[3] The temperature-induced transformations, however, are often less important compared to the superelasticity, which is an isothermal phenomenon and related to storage of potential energy. Self-expansion of stents, for example, is based on the superelasticity. The widely used SMA-based medical implants rely on further properties including corrosion resistance, biocompatibility and damping capacity. Therefore, NiTi-based SMAs are FDA approved for long-term implants.[4] The biocompatibility of NiTi is excellent as demonstrated for the numerous stents implanted so far, although nickel is known to have one of the highest potential for metal-induced allergies.[5-7] The well-prepared surface oxide, however, prevents the Ni release.[8] Hence, even porous NiTi constructs with a large surface area are expected to exhibit excellent biocompatibility in vitro and in vivo. [5,6]

*sebastian.friess@gloorinstruments.ch; phone 41 44 940-9955; fax 41 44 940-9914

Developments in X-Ray Tomography VII, edited by Stuart R. Stock, Proc. of SPIE Vol. 7804, 78041M · © 2010 SPIE · CCC code: 0277-786X/10/$18 · doi: 10.1117/12.861386

Selective laser melting (SLM) is an additive layer manufacturing technique, which allows for the fabrication of real parts from three-dimensional (3D) computer models. The technique already led to the production of fragile and complex-shaped constructs, difficult to be fabricated using other machining methods. SLM includes the spreading of metal powder on top of a building platform. A focused laser beam 'writes' the information of the selected slice of a 3D model into this powder layer. The laser treatment melts the powder, which subsequently solidifies. After such a process step, the building platform is replaced by about the thickness of the powder layer, and the next layer of powder is added. The processes are continued until the specimen has been finalized.

For the present investigation, SLM served for the fabrication of NiTi-specimens. These SMA-specimens exhibit the one-way shape memory effect, as schematically shown in Figure 1. This effect relates to the ability of the SMA material to recover its shape upon heating subsequent to pseudo-plastic deformation. This shape recovery was observed and quantified by means of conventional micro computed tomography (µCT). For this purpose, the specimen has been placed into a heating stage, which was incorporated into the µCT system. Thus, the non-deformed martensite state as well as the deformed martensite state were recorded at room temperature, the austenite state was recorded at elevated temperature. These three 3D datasets were registered to determine the strain field with micrometer precision in 3D space. Compared to optical detection, the role of pores in the deformation process can be uncovered. Therefore, µCT is especially supportive for the investigation of micro- and macro-porous SMA-constructs.

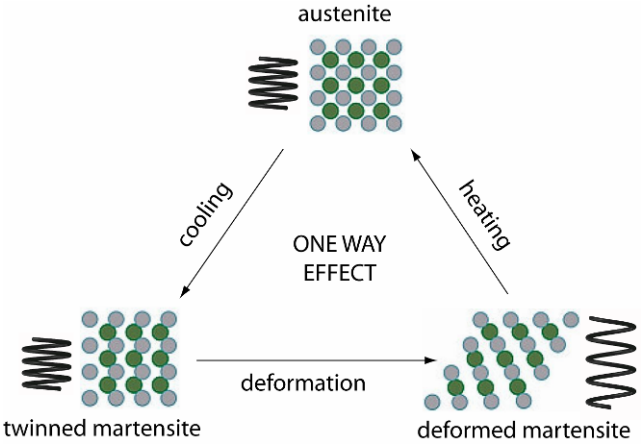

Figure 1. The schematic sketch shows the martensite-austenite phase transition for the one-way shape memory effect on macroscopic level (spring) and atomic level (green- and gray-colored balls) as well known for NiTi.

2. MATERIALS AND METHODS

The crystallographic structure of the SLM-fabricated NiTi specimen is mainly martensitic at room temperature, as can be derived from differential scanning calorimetry (DSC) measurements. NiTi-SMAs in martensitic state exhibit the shape memory effect. Within this preliminary investigation, a spiral spring between two plates was designed (see Figure 2) as it permits easy manual deformation of the construct. The starting situation (State I) refers to the original non-deformed martensitic phase at room temperature. State II refers to the expanded shape in the deformed martensite structure. State III corresponds to the shape recovery after heating above the austenite finish temperature A_f, which is the temperature of complete transition from martensite to austenite.

2.1 Specimen preparation

The selective laser melting of the NiTi specimens was performed by means of the SLM Realizer 100 (MTT Technologies, Lübeck, Germany) operated with a continuous wave Ytterbium-fiber laser with a wavelength between 1068 and 1095 nm. The basic raw material was pre-alloyed NiTi-powder (MEMRY GmbH, Weil am Rhein, Germany) with a d_{50}-value of 60 µm. According to Meier et al. the laser parameters were adjusted to an energy density E_v of 85 J/mm^3. [9] For that purpose, the laser power P_l, the layer thickness D_s, the scan velocity v_l and the hatch distance Δy_s were adapted in accordance with Equation 1. The powder layer thickness was set to 50 µm.

$$E_v = \frac{P_l}{\Delta y_s \cdot D_s \cdot v_l} \tag{1}$$

After fabrication, the specimens have been cleaned from adhering powder particles by compressed air and ultrasound. To reduce the internal stress resulting from the laser treatment in the spiral spring, the specimen was annealed at a temperature of 480 °C for 10 min in pure Ar atmosphere and cooled down to room temperature with a rate of 2 K/min. Finally, the spiral spring was (pseudo-)plastically expanded in the martensite phase.

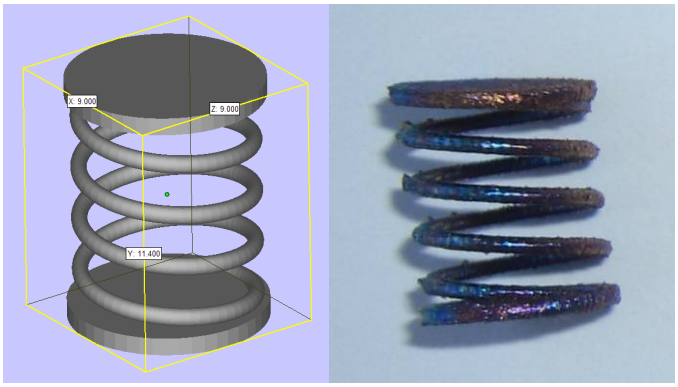

Figure 2. Computer model and a related photograph of the specimen fabricated by SLM. The spring fits into a rectangular volume of 9 mm × 9 mm × 11.4 mm.

2.2 Differential scanning calorimetry to characterize the phase transition

The transition temperatures of the NiTi-powder and of the SLM-structures were determined by DSC-measurements according to the ASTM standard[10]. The DSC 30 (Mettler-Toledo Intl. Inc.) was used to evaluate the thermal properties in the temperature range between -100 °C and 125 °C.

2.3 Micro computed tomography

The spiral spring (see Figure 2) and a porous cylinder about 3.5 mm in diameter were mounted on the SkyScan heating stage (see below) for tomography experiments with the SkyScan 1172™ high-resolution micro CT scanner (SkyScan NV, Kontich, Belgium), equipped with a 100 kV / 100 µA X-ray source and a 10 megapixel X-ray sensitive CCD camera. The system allows for a unique flexible geometry along the optical axis, i.e. the objects can be magnified until the boundaries of the field-of-view of the camera are reached. The specimens were individually 360°-scanned using an accelerating voltage of 100 kV and a beam current of 100 µA. In order to increase the mean photon energy, an Al/Cu filter was introduced. The spiral NiTi-spring was measured before and after deformation as well as before and after heating. The selected camera read-out (1000 × 524 pixels, 16-bit) resulted in an overall pixel size of 32.3 µm × 32.3 µm. For the NiTi-cylinder the camera read-out (2000 × 1048 pixels) led to an overall pixel size of 3.48 µm × 3.48 µm.

The reconstruction was carried out by the NRecon v1.6.1.2 software (SkyScan NV, Kontich, Belgium) that is based on a modified Feldkamp algorithm. It resulted in a set of 463 stacked slices with a dynamic range of 16-bit for the spiral spring and a set of 962 slices for the cylinder.

Thicker NiTi-cylinders (5 mm and 7 mm in diameter) have been scanned using the nano-tom™ (Phoenix x-ray, Wunstorf, Germany) equipped with a 180 kV / 15 W X-ray source. The cylinders were 360°-scanned using an accelerating voltage of 180 kV and a beam current of 33 mA. The X-ray beam was filtered by means of a 0.2 mm-thick Al-filter for the 7 mm cylinder and a 0.5 mm-thick Cu-filter for the 5 mm cylinder, respectively. The camera read-out, 2304 × 2304 pixels, resulted in a pixel length of 4 µm. The amount of data was reduced by binning with a factor 2.

2.4 Heating stage for µCT-system

SkyScan developed a dedicated heating stage for their µCT-system 1172™. This heating unit consists of a two-stage solid-state PELTIER heat pump to control the temperature of the specimen between room temperature and 80 °C. The microprocessor integrated at the bottom of the heating stage (see Figure 3) allows setting well-defined temperatures. The temperature sensor located directly at the copper support for the specimen provides the necessary feedback. The two fans

create a continuous airflow through the metallic cooling fins inside the stage's body in order to remove the heat from the PELTIER elements.

The spiral spring was mounted inside the heating stage on top of the copper piece (see Figure 3). A transparent polymer cap that is almost X-ray transparent surrounds the specimen to achieve a stable temperature regime during the tomography experiment.

Figure 3. Photograph of heating stage consisting of (1) microprocessor controller and power converter for the Peltier elements inside protective metal, (2) fans for air cooling, (3) square-shaped Peltier elements, (4) copper-made specimen support with temperature sensor element, (5) specimen holder, and (6) transparent polymer cap with sealing ring.[11]

2.5 Data treatment

For the visualization of the 3D data, we have applied the software VG Studio Max 2.0 (Volume Graphics, Heidelberg, Germany).

In order to determine the local deformations of the spiral spring in the different states the 3D datasets were registered, as it was done by German et al. for 2D data.[12] The affine registration yields the translational and rotational parameters to superimpose the center of gravity and to orient the axes of inertia as well as the three scaling factors along the selected three orthogonal axes. In case of the NiTi-spring we are interested in the scaling parameters, which characterize the macroscopic deformation. To identify, however, the strain distribution within the NiTi-specimen a non-rigid registration tool has to be used. We used the non-rigid registration algorithm introduced by Andronache et al., which is based on the adaptive hierarchical image subdivision strategy decomposing the non-rigid matching problem into numerous local rigid registrations of sub-images of decreasing size.[13] Prior to registration a threshold was set for the segmentation of material and air in between the well separated peaks. Registration of the datasets in affine and in non-rigid mode were performed utilizing the analyze file format. Calculation of the visualized strain field was done by Matlab 7.8 (MathWorks, Natick, USA).

3. RESULTS AND DISSCUSSION

3.1 Shape memory effect of NiTi powder and SLM specimen

The temperatures of the phase transitions from martensite to austenite and vice versa in the NiTi powder as well as in the produced SLM parts were determined by differential scanning calorimetry (DSC) as summarized in Figure 4. The transition temperatures are a function of the laser parameters used during fabrication.[14] The austenite and martensite peaks A_p and M_p are shifted to higher temperatures increasing the energy density, as shown in the right diagram of Figure 4. Hence, the phase transition temperatures can be tailored by the choice of the laser parameters.

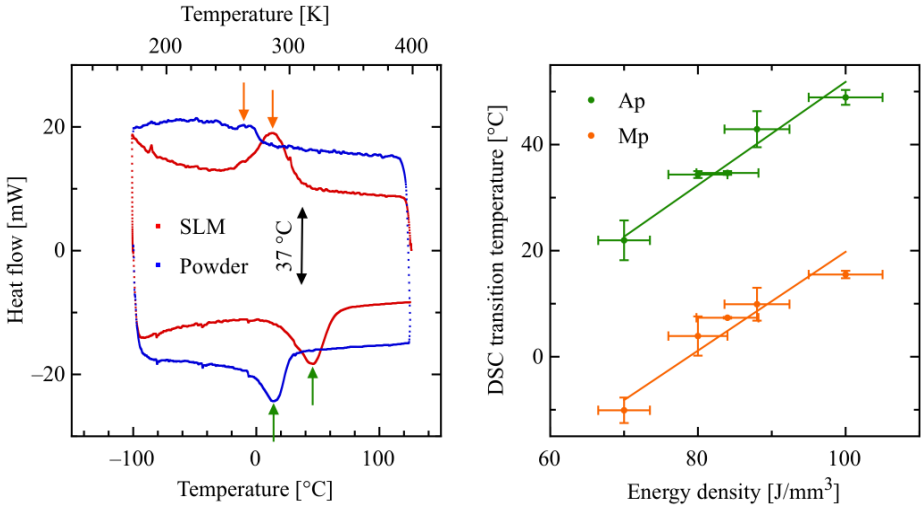

Figure 4. The DSC curves (left diagram) show different transition temperatures for the SMA-powder and the SLM-specimen. The right diagram demonstrates a linear dependence of the transition temperatures from the energy density of the laser beam for the rapid prototyping processes.

The spiral spring that is shown in Figure 5 as 3D representation from µCT-data exhibits its austenite peak temperature A_p at 46 °C (compare green-colored arrow of the red-colored curve in the left diagram of Figure 4). As also seen from the red-colored DSC curve in Figure 4, the offset value for the austenite transition lies at the temperature of about 75 °C. Heating of the NiTi-spring to a temperature of 80 °C therefore results in the complete transition into austenitic phase.

Figure 5 shows the shape memory effect of the NiTi spiral spring fabricated by SLM in qualitative manner. The left image shows the original state after SLM-processing. The image in the center represents the spring after pseudo-plastic deformation. The temperature increase of the spring in the heating stage of the µCT system above 80 °C results in a significant deformation towards the original state.

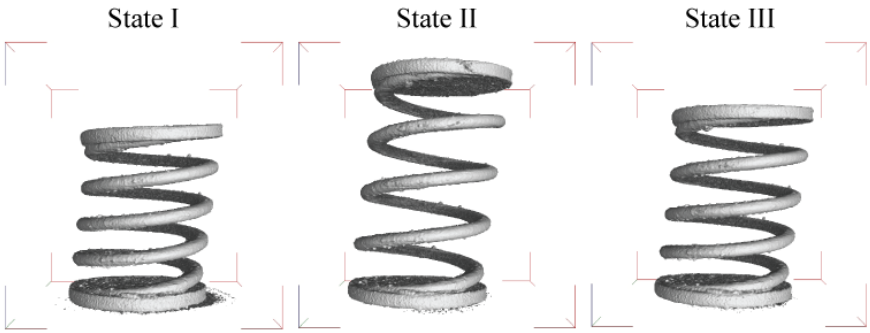

Figure 5. 3D representations of µCT-data from the spiral NiTi spring: Specimen as generated by SLM in cold state - martensite phase (left image), specimen after pseudo-plastic deformation (central image), and NiTi-specimen after shape recovered shape due to heating above transition temperature (right image).

3.2 Affine registration

To quantify the strain of the NiTi-spiral between of the different stages, the µCT-data were registered. The affine registration gives nine independent parameters. Six of them refer to the translation and rotation of a rigid body. Therefore, only the three remaining scaling parameters describe the strain of the spiral. Table 1 summarizes the scaling parameters. The scaling in x- and y-direction is close to unity, but the scaling in the z-direction, i.e. along the spiral axis, shows the expected shape memory effect of several 10%.

Table 1. Scaling factors resulting from the affine registrations between the tomography data. Note that the reference is always the tomography measurement done first.

Scaling factor	x-direction	y-direction	z-direction
State I – State II	1.00	1.00	0.72
State II – State III	1.00	0.99	1.26
State I – State III	1.00	1.00	0.90

One expects that States I and III are identical and the related scaling factor corresponds to unity. The specimen in the recovered state (State III), however, has to be scaled by a factor of 0.9 in z-direction to reproduce the original state. The specimen does not completely recover, as qualitatively seen in the images of Figure 5. The reason for the incomplete shape recovery might be the imperfect heat conductance between the NiTi-spiral and the sample holder. This hypothesis is supported by the fact that the heat transfer from heating stage to the entire specimen takes place via the copper piece. Especially the contact between specimen and copper holder seems to be a critical issue as the base of the specimen is rough.

The scaling factors in the x- and y-directions are close to unity. This is somehow surprising, since one expects a decrease in spiral diameter as the result of expansion. The presence of the two plates at the bottom and the top of the spiral wire, however, prevents the detection of this phenomenon using the affine registration tool.

Since only one parameter can be selected for the scaling in the z-direction, the cross-section of the spiral wire becomes an elliptical shape that is not observed in the tomography data. Therefore, the affine registration tool is only a rough estimate, which does not account for the deformation of the SMA-specimen on the micrometer scale.

3.3 Non-rigid registration

In order to quantify the entire 3D strain field of the NiTi-spiral between of the different stages, the µCT-data were non-rigidly registered. The results are represented in Figure 6 by color-coded virtual cuts. The reference is always the dataset measured first. Consequently, the colors relate to the subsequent deformation and displacement, respectively. The color represents the amount of the local displacement vector for each voxel present in the NiTi-specimen.

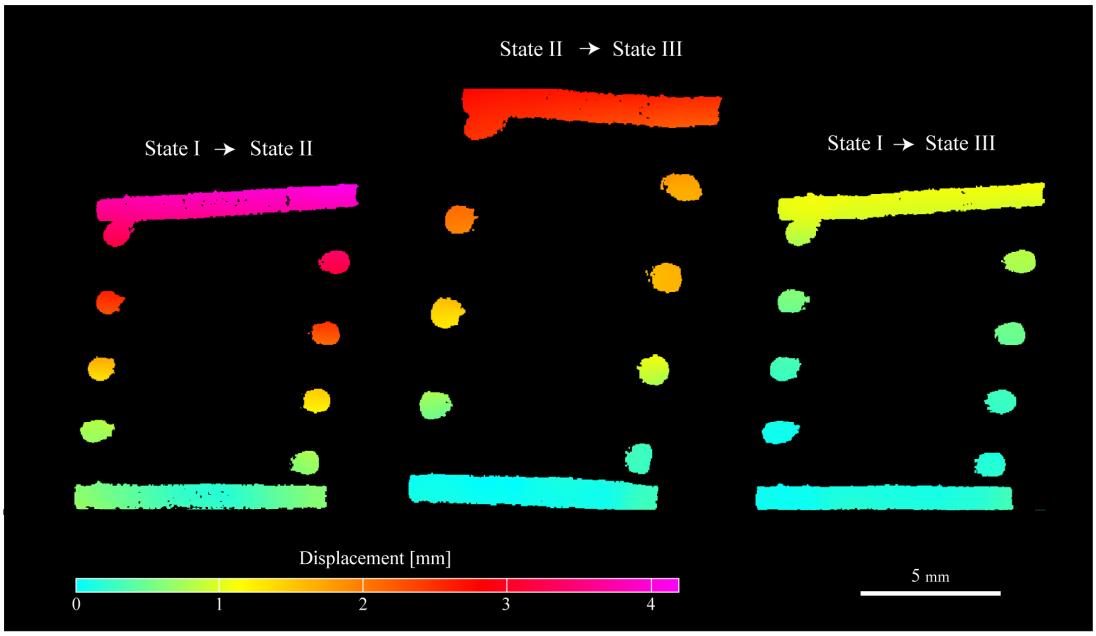

Figure 6. Strain fields of the spiral spring after shape changes from State I to State II, State II to State III and State I to State III. The amount of the displacement vector is color-coded shown on the virtual cuts through the spiral spring connected to the top and bottom plates.

The spiral specimen is more or less uniformly deformed (State I → State II), which is seen from the regular increase in the displacement over the turns of the spiral.

If one compares the original shape (State I) with the resulting shape in State III, it is clearly visible that the displacement is not fully symmetric between top and bottom plates. The top of the specimen exhibits still a displacement of about 1 mm whereas the bottom is hardly displaced at all. This finding supports the hypothesis that the incomplete shape recovery results from temperature gradients along the z-axis of the spiral.

3.4 Pores in SLM-fabricated SMA-rods

SLM-fabricated metal constructs often contain micro-pores, which can significantly alter the mechanical properties of such products. Therefore, SMA-rods fabricated by means of SLM were characterized using high-resolution µCT. Figure 7 shows virtual cuts through 3D data of such rods with diameters between 3.5 and 7 mm. Pores of micrometer sizes are clearly identified. On first glance, they are homogeneously distributed over the bulk. A deeper insight into the local distribution, however, reveals a higher density of pores near the support structure, as seen best in the cuts parallel to the symmetry axis. An even higher density of pores is uncovered within the support material, i.e. to the material, which connects the structure of interest with the building platform (cp. Figure 7 b).

This preliminary experiment demonstrates that µCT using the nano-tom™ and the SkyScan 1172^{TM}, respectively, allows studying the pore density and distribution as done for example by Fierz et al. and Mueller et al..[15,16] This will benefit the optimization of the SLM process selecting the appropriate fabrication parameters in an iterative way.

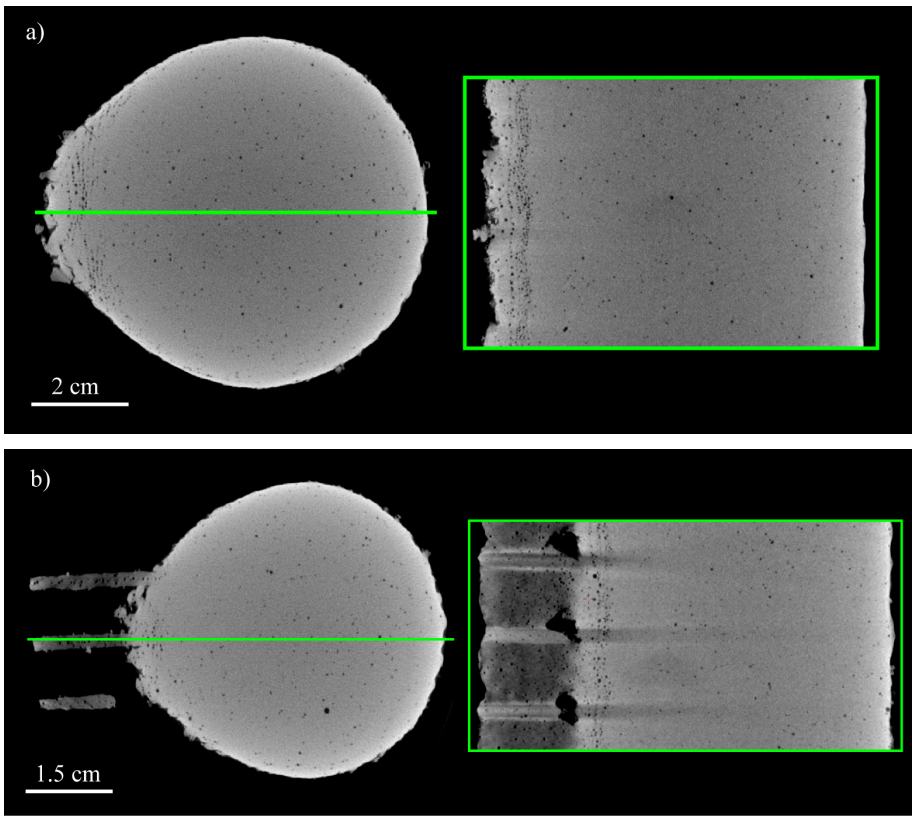

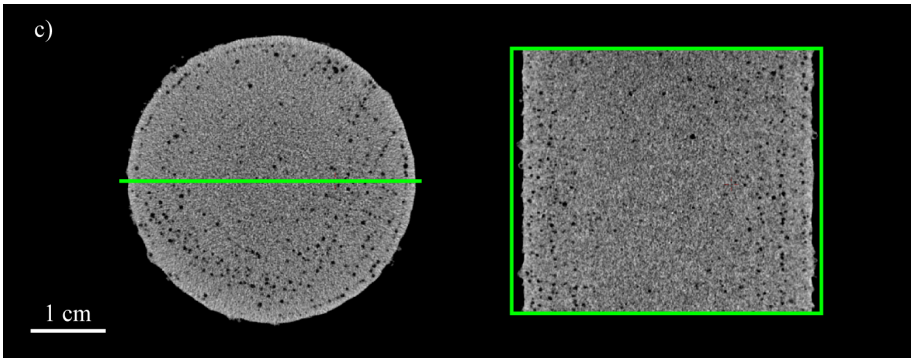

Figure 7. Virtual cuts parallel and perpendicular to the symmetry axis of the rods and directions of fabrication, respectively, to visualize the micro-pore distribution and density in NiTi specimens fabricated by means of SLM.

4. CONCLUSIONS

The SkyScan heating stage is a useful instrumentation for investigations on the shape memory effects in NiTi specimens. The different states of the shape memory effect could be visualized and quantitatively evaluated by affine and non-rigid registrations of the tomography data. The induced pseudo-plastic deformation could be mainly reversed heating the NiTi structure up to 80 °C. A deformation of approximately 10% remains, which is presumably the result of the limited heat transfer between the sample stage and the rough bottom of the specimen. This problem should be mastered increasing the time period of pre-heating or, even better, improving the thermal connection between specimen and copper piece of the heating stage.

A deep insight into the deformation mechanisms upon the shape memory effect in complex microstructures is gained applying non-rigid registration tools to μCT data of NiTi constructs. This feedback is extremely helpful for the optimization of the design and the fabrication procedure of complex shaped SMA-based, medical implant systems.

ACKNOWLEDGEMENTS

The multi-disciplinary team gratefully acknowledges F. Beckmann and U. Pieles for technical support as well as Sh. Mushkolaj for the image in figure 1. Furthermore the authors thank for the financial support of the Swiss National Science Foundation for the project entitled “Porous shape-memory-scaffolds as mechanically active bone implants” within the program NRP 62 ‘Smart Materials‘.

REFERENCES

[1] Kaack, M., "Elastische Eigenschaften von NiTi-Formgedächtnis-Legierungen", Ruhr-Universität Bochum, Bochum (2002).

[2] Allafi, J.K., "Mikrostrukturelle Untersuchungen zum Einfluss von thermomechanischen Behandlungen auf die martensitischen Phasenumwandlungen an einer Ni-reichen NiTi-Formgedächtnislegierung", Ruhr-Universität Bochum, Bochum (2002).

[3] Müller, B., H. Deyhle, S. Mushkolaj, and M. Wieland, "The challenges in artificial muscle research to treat incontinence", Swiss Medical Weekly 30-40, (2009).

[4] ASTM Standard, "Standard Specification for Wrought Nickel-Titanium Shape Memory Alloys for Medical Devices and Surgical Implants", ASTM Standard F2063, (2005).

[5] Es-Souni, M., M. Es-Souni, and H. Fischer-Brandies, "Assessing the biocompatibility of NiTi shape memory alloys used for medical applications", Anal Bioanal Chem 381, 557-567 (2005).

[6] Prymak, O., D. Bogdanski, M. Koller, S.A. Esenwein, G. Muhr, F. Beckmann, T. Donath, M. Assad, and M. Epple, "Morphological characterization and in vitro biocompatibility of a porous nickel-titanium alloy", Biomaterials 26(29), 5801-7 (2005).

[7] Stoeckel D, B.C., Duda S. A, "Stoeckel D, Bonsignore C, Duda S. A survey of stent designs. " Minimally Invasive Therapy & Allied Technologies 11(4), 137-147 (2002).
[8] Shabalovskaya, S.A., H. Tian, J.W. Anderegg, D.U. Schryvers, W.U. Carroll, and J. Van Humbeeck, "The influence of surface oxides on the distribution and release of nickel from Nitinol wires", Biomaterials 30(4), 468-77 (2009).
[9] Meier, H., C. Haberland, J. Frenzel, and R. Zarnetta, "Selective Laser Melting of NiTi shape memory components", in: Innovative Developments in Design and Manufacturing. 2010, Taylor & Francis Group: London. p. 233-238.
[10] ASTM Standard, "Standard Test Method for Transformation Temperature of Nickel-Titanium Alloys by Thermal Analysis", ASTM Standard F2004, (2004).
[11] "SkyScan cooling and heatung stages for the SkyScan 1172, 1173 and 1174 micro-CT systems ", Editor: SkyScan ™, Kontich (2010).
[12] Germann, M., A. Morel, F. Beckmann, A. Andronache, D. Jeanmonod, and B. Muller, "Strain fields in histological slices of brain tissue determined by synchrotron radiation-based micro computed tomography", J Neurosci Methods 170(1), 149-55 (2008).
[13] Andronache, A., M. von Siebenthal, G. Szekely, and P. Cattin, "Non-rigid registration of multi-modal images using both mutual information and cross-correlation", Medical Image Analysis 12, 3-15 (2008).
[14] Bormann, T., R. Schumacher, B. Müller, M. Mertmann, U. Pieles, and M. de Wild, "Properties of NiTi-Structures Fabricated by Selective Laser Melting", eCells and Materials Journal 20 Supplement 1, 13 (2010).
[15] Müller, B., F. Beckmann, M. Huser, F. Maspero, G. Szekely, K. Ruffieux, P. Thurner, and E. Wintermantel, "Non-destructive three-dimensional evaluation of a polymer sponge by micro-tomography using synchrotron radiation", Biomol Eng 19(2-6), 73-8 (2002).
[16] Fierz, F.C., F. Beckmann, M. Huser, S.H. Irsen, B. Leukers, F. Witte, O. Degistirici, A. Andronache, M. Thie, and B. Muller, "The morphology of anisotropic 3D-printed hydroxyapatite scaffolds", Biomaterials 29(28), 3799-806 (2008).